AFRL-AFOSR-VA-TR-2024-0061

Advanced Cooling Technologies, Inc.

WILLIAM ANDERSON
ADVANCED COOLING TECHNOLOGIES INC
1046 NEW HOLLAND AVENUE
LANCASTER, PA, 17601-5606
US

12/07/2023
Final Technical Report

Air Force Research Laboratory
Air Force Office of Scientific Research
Arlington, Virginia 22203
Air Force Materiel Command

REPORT DOCUMENTATION PAGE

PLEASE DO NOT RETURN YOUR FORM TO THE ABOVE ORGANIZATION.

1. REPORT DATE	2. REPORT TYPE	3. DATES COVERED	
20231207	Final	START DATE 20230301	END DATE 20230831

4. TITLE AND SUBTITLE
Advanced Cooling Technologies, Inc.

5a. CONTRACT NUMBER	5b. GRANT NUMBER	5c. PROGRAM ELEMENT NUMBER
FA9550-23-P-0002		61102F
5d. PROJECT NUMBER	**5e. TASK NUMBER**	**5f. WORK UNIT NUMBER**

6. AUTHOR(S)
William Anderson

7. PERFORMING ORGANIZATION NAME(S) AND ADDRESS(ES)	8. PERFORMING ORGANIZATION REPORT NUMBER
ADVANCED COOLING TECHNOLOGIES INC 1046 NEW HOLLAND AVENUE LANCASTER, PA 17601-5606 US	

9. SPONSORING/MONITORING AGENCY NAME(S) AND ADDRESS(ES)	10. SPONSOR/MONITOR'S ACRONYM(S)	11. SPONSOR/MONITOR'S REPORT NUMBER(S)
Air Force Office of Scientific Research 875 N. Randolph St. Room 3112 Arlington, VA 22203	AFRL/AFOSR RTB1	AFRL-AFOSR-VA-TR-2024-0061

12. DISTRIBUTION/AVAILABILITY STATEMENT
A Distribution Unlimited: PB Public Release

13. SUPPLEMENTARY NOTES

14. ABSTRACT
For Phase I, the laser diagnostics, we propose to develop, includes Planar Laser Induced Fluorescence (PLIF) imaging measurements of quantitative species concentration over the substrate surfaces. This will be combined with emission spectrum measurements and temperature measurements. 2D measurements of O atoms will be measured by Two-Photon Absorption Laser Induced Fluorescence (TALIF) over a substrate (ceramic and metal tubes/rods) surface. Temperatures close to the surface will be measured by NO LIF measurements.

15. SUBJECT TERMS

16. SECURITY CLASSIFICATION OF:			17. LIMITATION OF ABSTRACT	18. NUMBER OF PAGES
a. REPORT	b. ABSTRACT	c. THIS PAGE		
U	U	U	UU	38

19a. NAME OF RESPONSIBLE PERSON	19b. PHONE NUMBER *(Include area code)*
JOHN LUGINSLAND	000-0000

Standard Form 298 (Rev.5/2020)
Prescribed by ANSI Std. Z39.18

AF SBIR Phase I
Award # FA9550-23-P-0002

Laser-based diagnostic for plasma-surface interactions
Month 6 (August 2023) Report

Prepared By:
Dr. Mruthunjaya Uddi, PI (ACT)
Prof. Arthur Dogariu (TAMU)
Mr. Gerardo Urdaneta (TAMU)
Mr. James Montoya (TAMU)

Advanced Cooling Technologies, Inc.
1046 New Holland Avenue
Lancaster, PA 17601

Program Manager
Dr. John Luginsland

March 1, 2023 – November 30, 2023

Table of Contents

1. Summary

This document consists of the summary Phase I program entitled, "Laser-based diagnostic for plasma-surface interactions," Contract FA9550-23-P-0002. This status report contains the work performed during the period from May 1st, 2023, until June 30th, 2023. The AF Program Manager for this project is Dr. John Luginsland. The Principal Investigator for this project is Dr. Mruthunjaya Uddi from Advanced Cooling Technologies, Inc. (ACT). The subcontractor for this project is Prof. Arthur Dogariu, Texas A & M University (TAMU) and the consultant is Dr. Mark Sowa (Plasma ALD LLC.). ACT will design the experiments under the guidance of Dr. Sowa. The laser diagnostics studies will be conducted at TAMU under the guidance of Prof. Dogariu and Dr. Uddi.

The research team propose to develop and use spatially (<10 μm) and temporally (< 10 ns) resolved laser diagnostics to study plasma-surface interactions in an environment for Plasma-Enhanced Atomic Layer Deposition (PEALD) of crystalline films and Plasma-Enhanced Atomic Layer Etching (PEALE). This will enable the development of PEALD/PEALE for various applications including the coating of deep UV mirrors on satellites for astronomy, fabrication of semiconductors with atomic scale precision and other electrical-optical-thermal devices. PEALDPEALE methods can reduce adsorption and scattering in optical films because of the lower concentration of impurities, increased stoichiometric control, yielding vastly superior film deposition crystal quality and performance at lower deposition temperatures compared to traditional thermal Atomic Layer Deposition (ALD) techniques[1]. Deposition of a greater number of materials have been demonstrated using PEALD as compared to just ALD.

For Phase I, the laser diagnostics, we propose to develop, includes Planar Laser Induced Fluorescence (PLIF) imaging measurements of quantitative species concentration over the substrate surfaces. This will be combined with emission spectrum measurements and temperature measurements. 2D measurements of O atoms will be measured by Two-Photon Absorption Laser Induced Fluorescence (TALIF) over a substrate (ceramic and metal tubes/rods) surface. Temperatures close to the surface will be measured by NO LIF measurements.

Feedback from Air Force will be sought for continuous development of a detailed research plan for Phase II. Tentatively, we plan to conduct more detailed measurements of species such as O, F and N atoms, CO molecule by TALIF during Phase II. Plasma radicals such as OH, CH, NH can be measured by single photon Laser Induced Fluorescence (LIF). Methods to measure electron and ion fluxes, ion directionality and energy distributions will also be explored. Ions of interest are $\boldsymbol{O_2^-, O_2^+, O^+, O^-}$. Coatings deposited by PEALD will be characterized by methods such as SEM, XRD, EDS imaging etc.

Many species which are important in plasma processing applications (e.g., $\boldsymbol{BF_2^+}$, $\boldsymbol{C_xH_yF_z^+}$, $\boldsymbol{SiO_xC_yF_z}$, $\boldsymbol{COF}$) lack excitation transitions at easily accessible wavelengths, or the excited states do not fluoresce (often the case for larger polyatomic radicals). Therefore, the data needed includes the identification of transitions suitable for LIF of species relevant to plasma processing, the transition strength (Einstein A coefficient), and the fluorescence yield. This will the focus of Phase II efforts.

2. Research objectives:

The overall technical objective of the Phase I and Phase II efforts is to design, develop, and implement a compact integrated NDE optical-laser diagnostics system to measure chemical species and temperature close to a substrate, with high time (< 10 ns) and spatial resolution (< 10 μm) for repeatable, high-quality control of PEALD process. This will help study of plasma-surface interactions to enable development of advanced PEALD processes. Laser diagnostics to measure species concentrations such as O, N, F atoms, plasma generated radicals such as OH, CH, NH etc. and their energies with spatial and time resolution will enable better understanding and correlation to the PEALD finish quality.

The temperature measurement is another control parameter for the PEALD process and help in understanding the plasma-surface interaction physics. The plasma emission spectrum measurements can complement the species concentration measurements to give additional information about the PEALD physics and enable feedback control. Rotational-vibrational temperatures of species give insight into the physics and help develop strategies for PEALD process control. PEALD of thin films such as TiO_2 and InN will be studied in Phase II.

Towards these overall goals, the Phase I objectives can be summarized as:

Objective 1: Demonstrate spatially (2D) and time resolved measurements of O atoms over a substrate.

Objective 2: Demonstrate plasma emission measurements over a substrate and correlate with O atom concentration measurements.

Objective 3: Demonstrate 2D map temperature measurements over a substrate using NO Planar Laser Induced Fluorescence (PLIF) imaging.

Objective 4: Study detailed methods and smart strategies to measure concentrations of plasma chemical species and temperature for phase II efforts.

3. Project Schedule

The planned Phase I schedule is presented in Table 1. The Phase I program will last six months and consist of six technical tasks and a reporting task.

Table 1: Phase I Program Schedule

Task	Months					
	1	2	3	4	5	9
Task 1: Design of low-pressure plasma chamber with optical windows						
Task 2: Assembly of plasma chamber						
Task 3: Alignment of lasers and camera for O atom TALIF						
Task 4: O atom TALIF 2D imaging and concentration quantification						
Task 5: 2D NO concentration measurements by PLIF imaging						
Task 6: Plasma emission measurements						
Task 7: Reporting and Briefings						
Progress Reports	X	X		X		
Draft Final Report						X
Final Report						X

4. Accomplishments (Month 1 to 9)

The measurements proposed in the original proposal have been completed and the results are described in the following sections.

5. Reactor design and assembly

A quartz reactor based on plasma generated by an RF power system, and a flow system were designed (Fig. 1).

Fig. 1 shows the flow system design. The system is designed to flow air over the substrate. Two valves, pin valve and a butterfly valve, on the upstream and downstream side of the reactor, respectively, will enable control of both pressure and air flow rate. The mass flow meter can read air flow rates in the range 1-10 sccm. The pressure range of interest for experiments is 1- 10 mTorr.

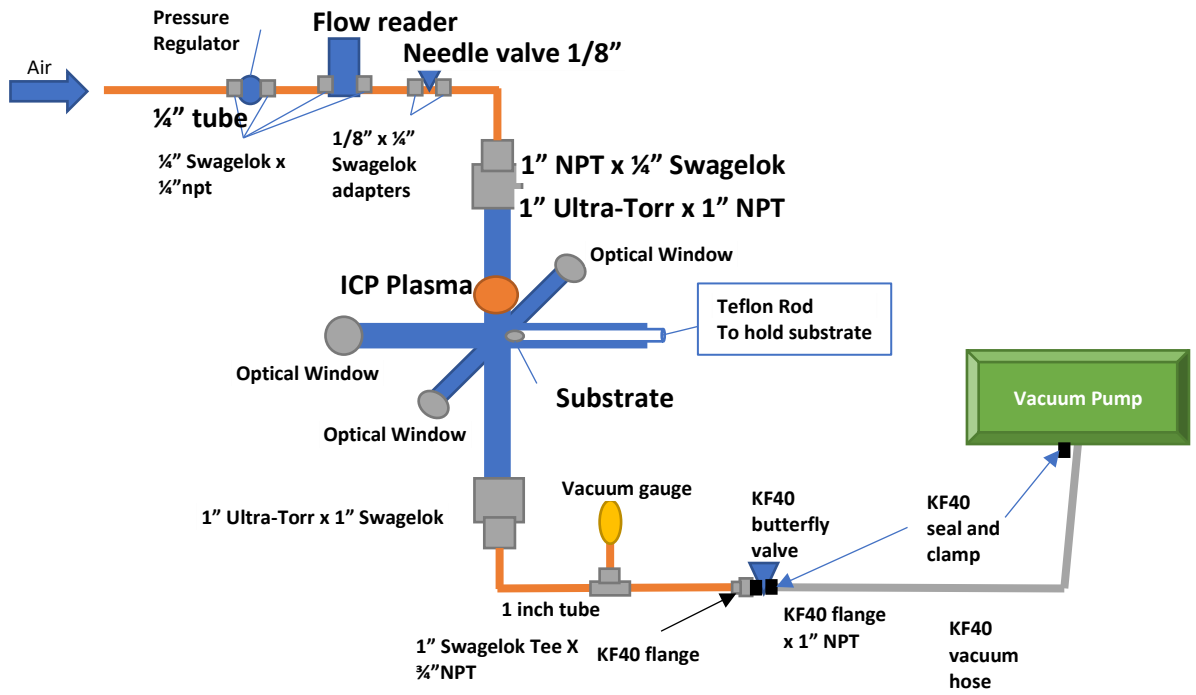

Figure 1: Schematic of flow system design through the reactor

Figs. 2-3 shows the design drawings of quartz reactor and optical windows. The ICP reactor is made of quartz with 4 in-plane tube arms (~1” length) and 2 perpendicular tube arms along the flow direction. The tube OD is 25 mm with wall thickness of ~ 1.58 mm. The optical windows are made of Swagelok ultratorr adaptors, with 1” diameter quartz optical windows bolted to one side of the adaptor using an O ring gasket.

Fig. 4 shows the pictures of the quartz reactor and the fabricated optical windows.

Fig. 5 shows cross section schematic of various substrates of interest. The substrates will be of electrical-thermal insulating (ceramic) and conductive (metal). Alumina ceramic tubes 1/16” OD with stainless steel rods inside them will be used as ceramic substrates. The steel rods can be connected to RF bias voltage to study the effect on time resolved measured species concentration over the substrate. Two ceramic rods can be oppositely biased using RF as shown in Fig. 7b. Fig. 7c-d show two types of metal substrates rods which can be biased with either RF or DC voltages. The peak bias voltage will be < 200 V^2.

Fig. 6 shows the assembly of the reactor in the initial stages of assembly. The ICP connection is not shown. 1/8” OD copper tubing wound into a spiral around the neck of the quartz tube just above the substrate will be used to generate the ICP. The tube can also be connected to water cooling flow using Swagelok adaptors.

The reactor was tested for air leakage. A low pressure of 3 mTorr or better was achieved.

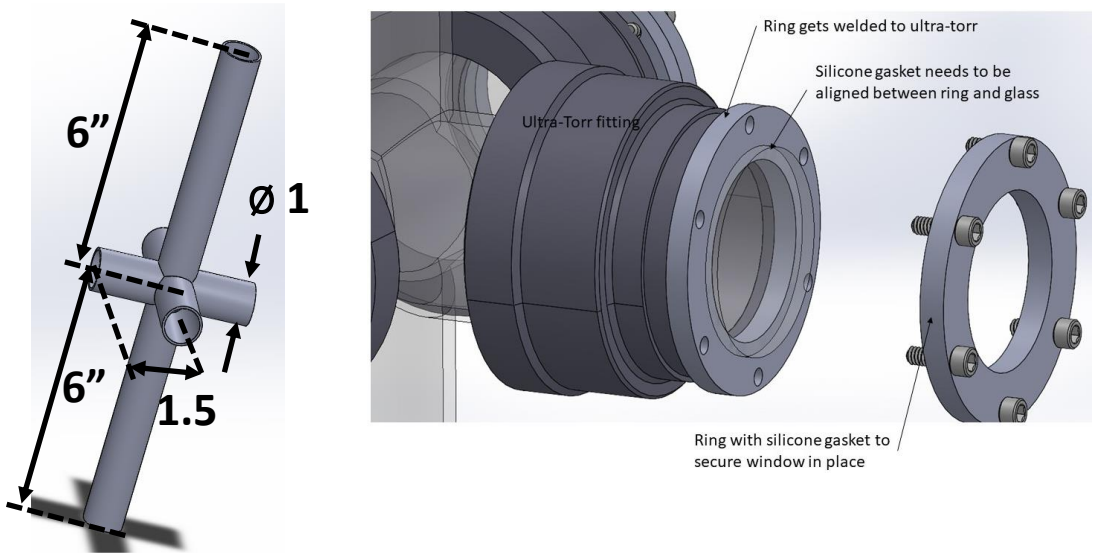

Figure 2: Drawings of the quartz reactor section (left) and optical window design (right).

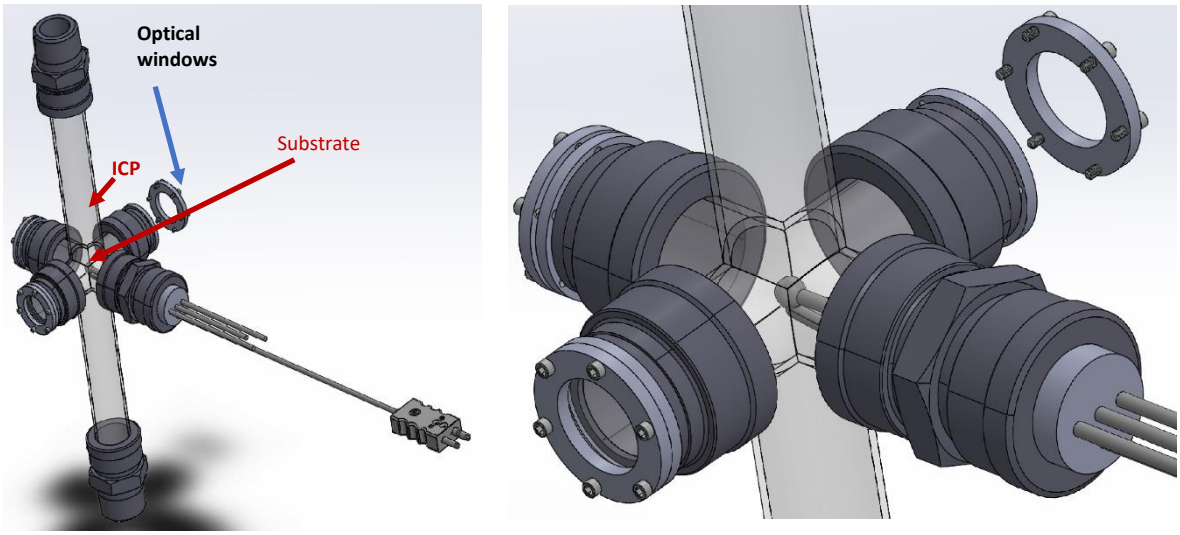

Figure 3: Drawings of the quartz reactor assembly (left) and optical windows (right).

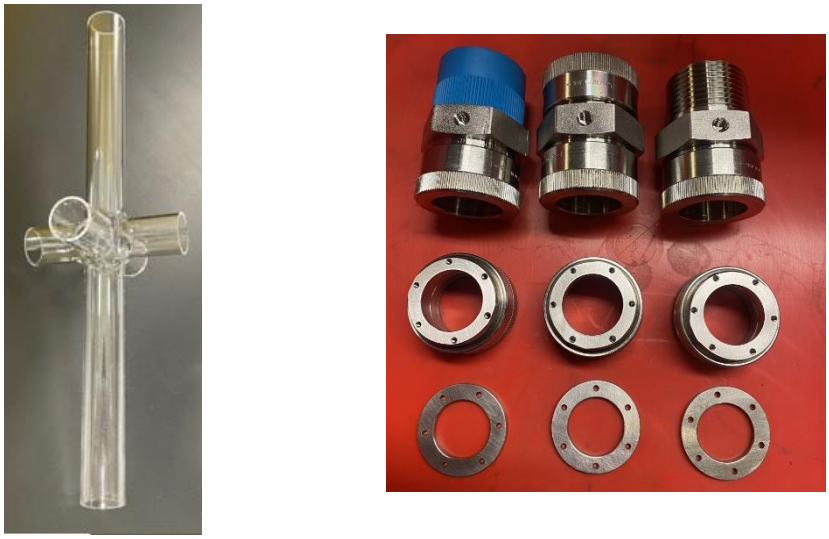

Figure 4: Pictures of the quartz reactor section (left) and optical windows (right).

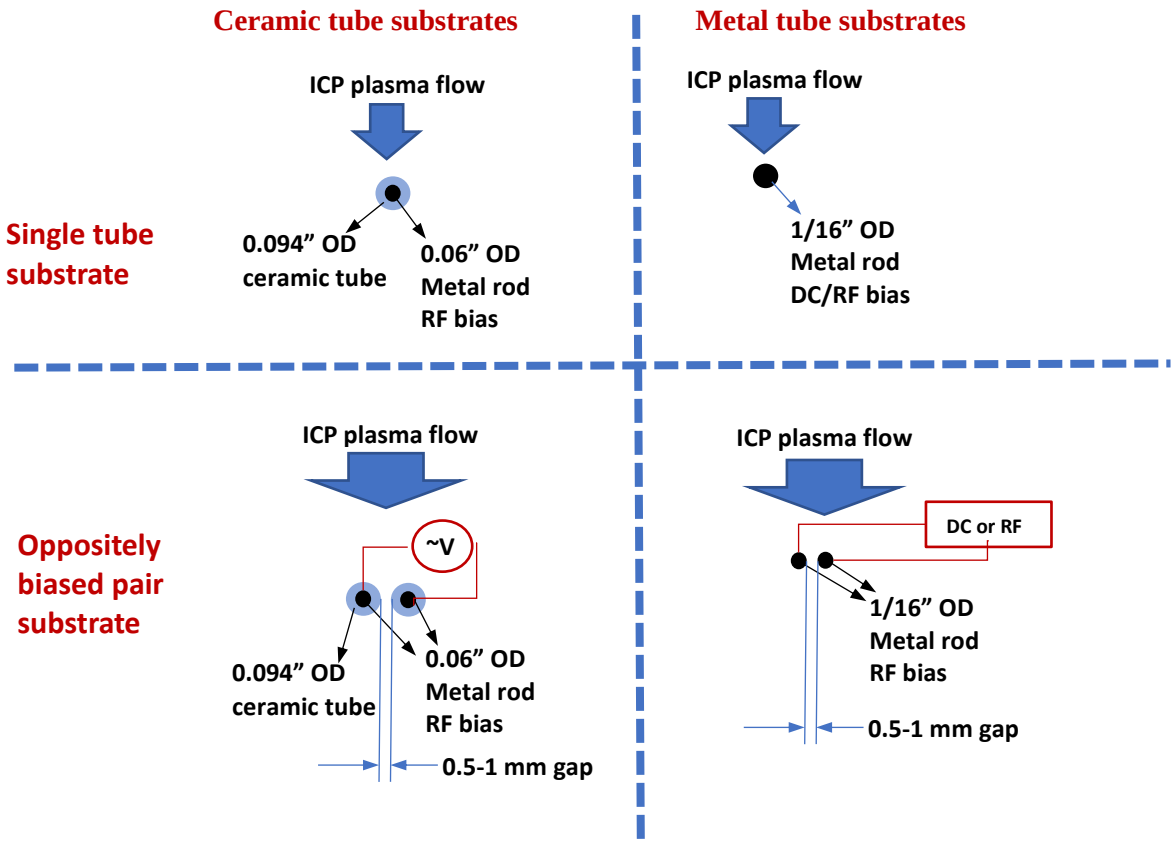

Figure 5: Cross section drawings of 4 types of substrates used for the studies. The substrates were placed in the path of the plasma. Laser diagnostics of the gas phase was conducted over the surfaces.

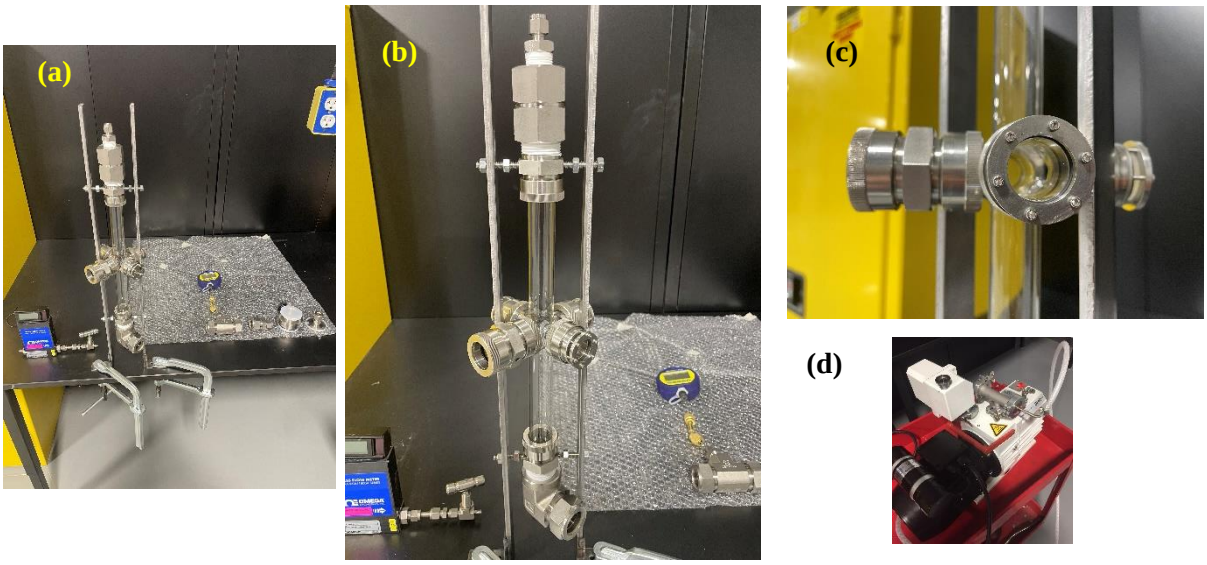

Figure 6: Picture of the quartz reactor assembly under test for vacuum and leakage. (a,b) assembly; (c) optical windows; (d) pump used.

6. Laser diagnostics approach

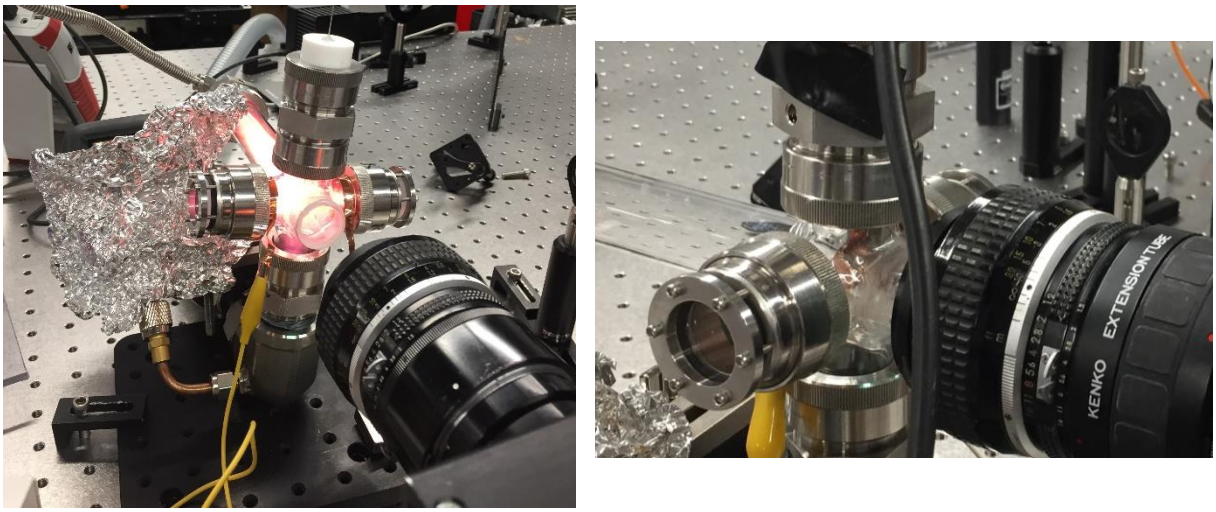

Figure 7: Picture of the quartz reactor assembly under test for vacuum and leakage. (a,b) assembly; (c) optical windows; (d) pump used.

Figure 7 shows the final assembly of the reactor with capacitively coupled RF discharge plasma. The substrate was used as one of the electrodes (active).

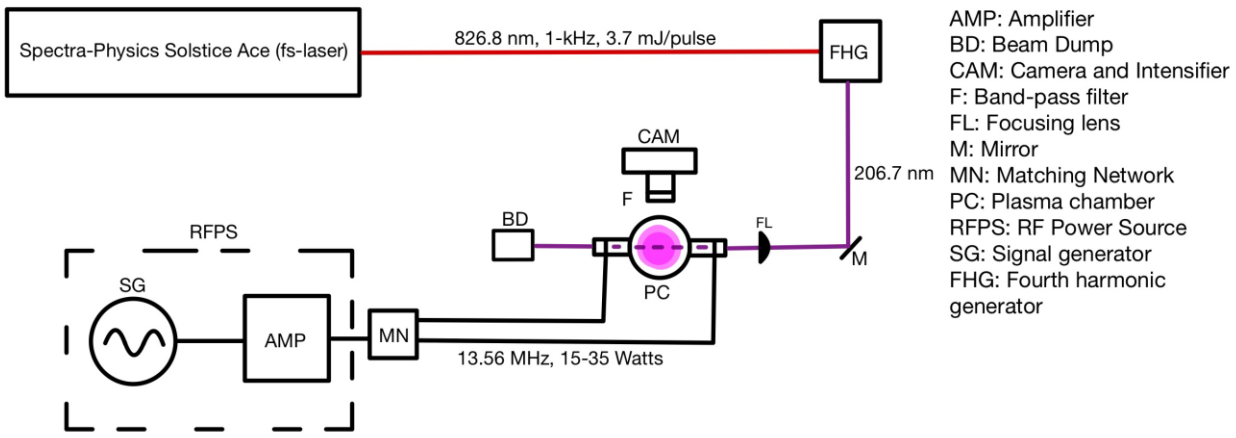

Figure 8: A tunable femtosecond (fs) laser at Texas A & M University was used to generate UV pulsed laser beam in the UV region (206 nm-227 nm) for LIF excitation of O and N atoms, NO molecule.

Figure 8 shows a schematic of the tunable fs-laser setup at TAMU used for LIF measurements. Figure 9 shows the 2-photon excitation and fluorescence scheme of the various atoms: Kr, H, N, Xe, O. The fluorescence emission wavelength for these atoms is different from the laser excitation wavelength. This enables use of bandpass optical filters to collect LIF signals while blocking laser scatter from the solid substrate surfaces. Kr 100ppm with balance air and Xe 1% mole fraction with balance air was used to calibrate N and Xe atom concentrations in plasma, respectively.

Figure 10 shows sample N atom TALIF images the laser grazing over the metal substrate surface.

At higher pressures (500 mTorr-1100 mTorr), non-uniform plasma (Figure 11 left) was obtained around both metal and ceramic substrates.

Figure 10 (right) shows an example O atom TALIF image with laser grazing over the metal substrate surface tangentially. All data was obtained with laser incident in this way over the substrate surface.

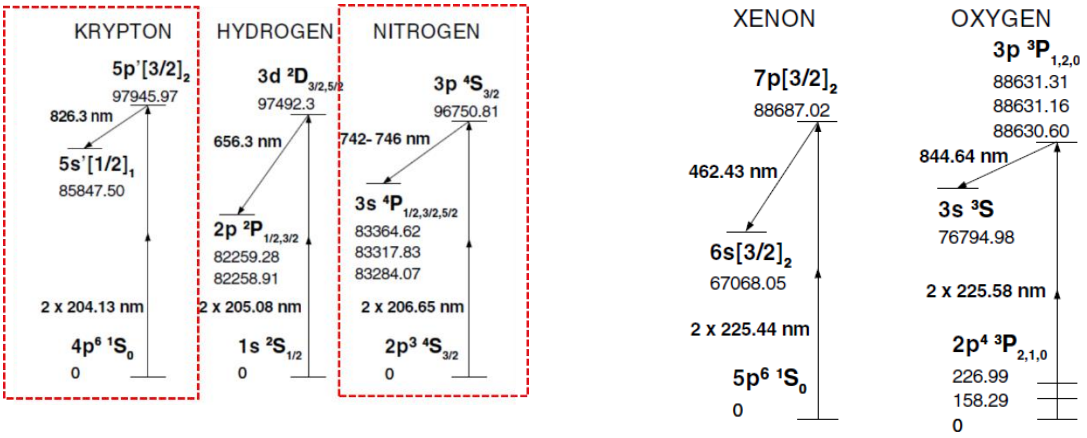

Figure 9: Two-photon excitation scheme for Kr, H, N, Xe and O atoms. The level energies are given in cm^{-1}.

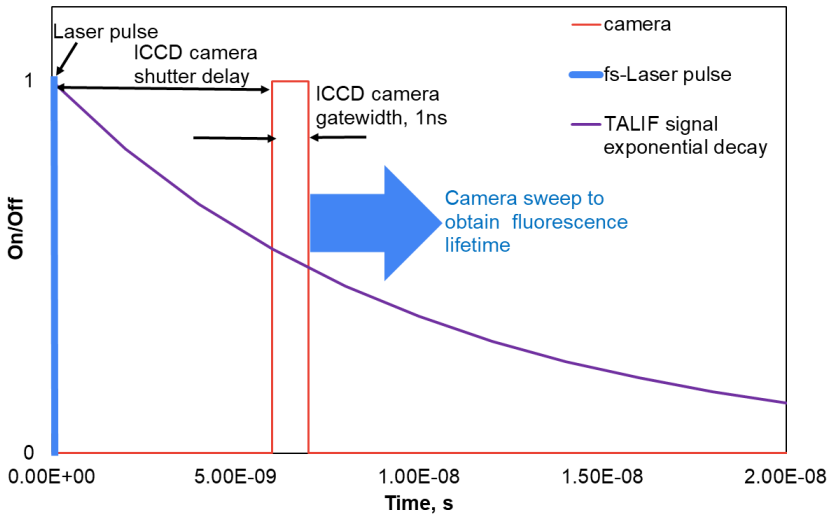

Figure 10: Schematic showing synchronization and timing of the fs-laser pulse and the camera gatewidth. The camera gate can be translated w.r.t. the laser pulse in time, to obtain fluorescence lifetime.

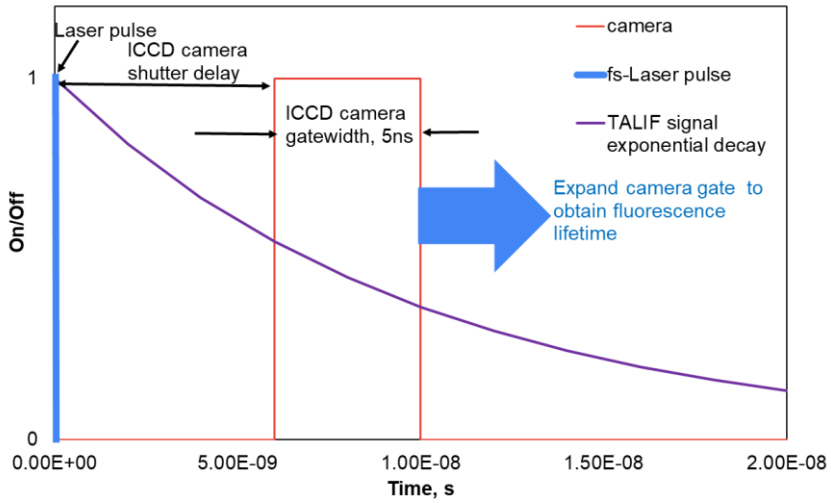

Figure 11: Schematic showing synchronization and timing of the fs-laser pulse and the camera gatewidth. The camera gate can also be expanded to collect the complete fluorescence signal over the lifetime.

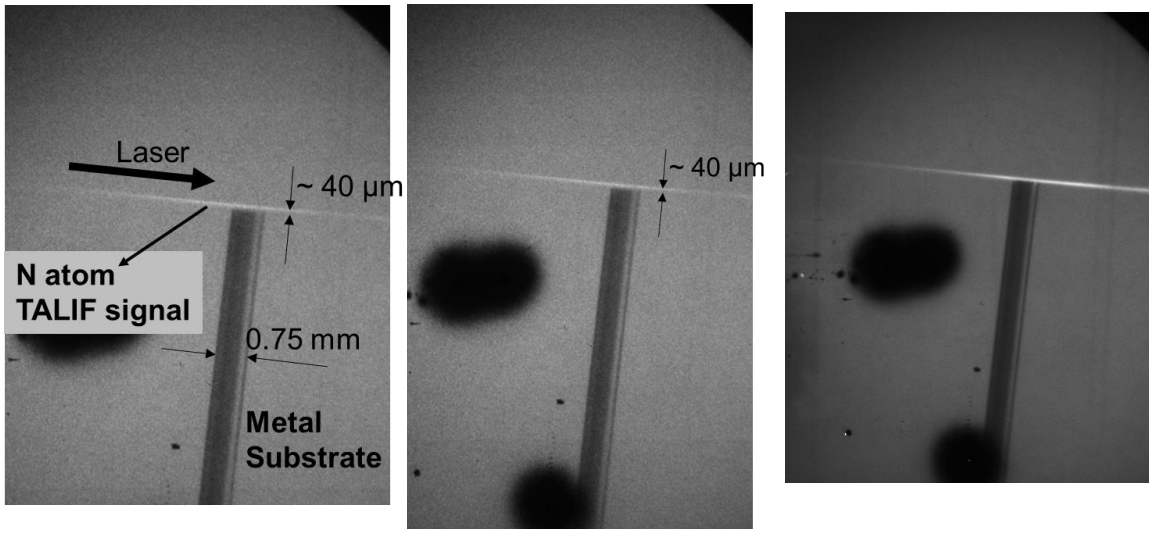

Figure 12: Example N atom TALIF images with laser grazing over the metal (ϕ750 µm) surface, 3 mTorr air.

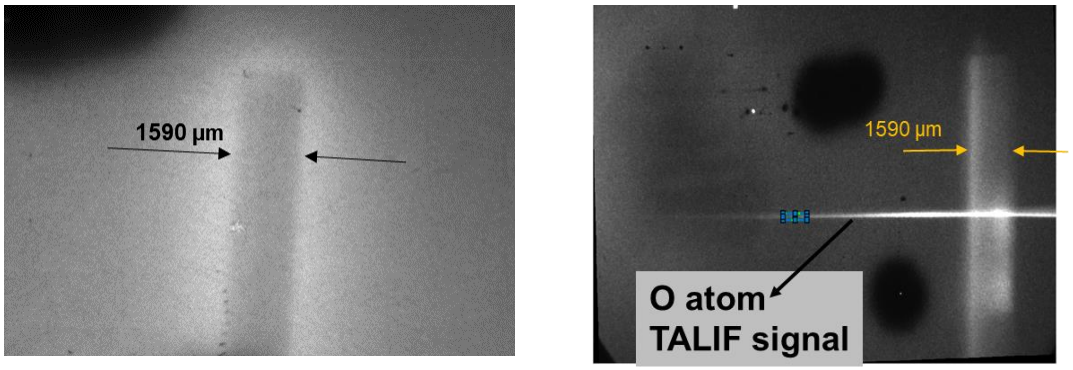

Figure 13: (left) Plasma emission around a metal substrate. At higher pressures (500 mTorr-1100 mTorr), non-uniform plasma was obtained around both metal and ceramic substrates.

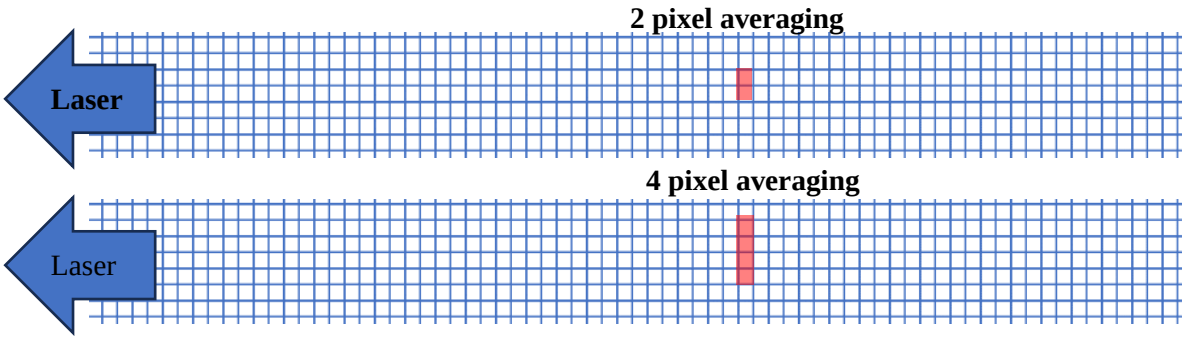

Figure 14: Planar TALIF and LIF signal can be averaged in different ways as shown in above two examples. The spatial resolution in our imaging was ~ 5.88 µm/pixel. Averaging over more pixels leads to better signal to noise ratio but compromises the spatial resolution.

Figure 15: A Kanthal wire heater rated up to 1200 ºC was used as a substrate. The metal substrate on the left was replaced with wire heater and thermocouples. 4-bore Ceramic tubes (1/4" OD) were used to make the connections.

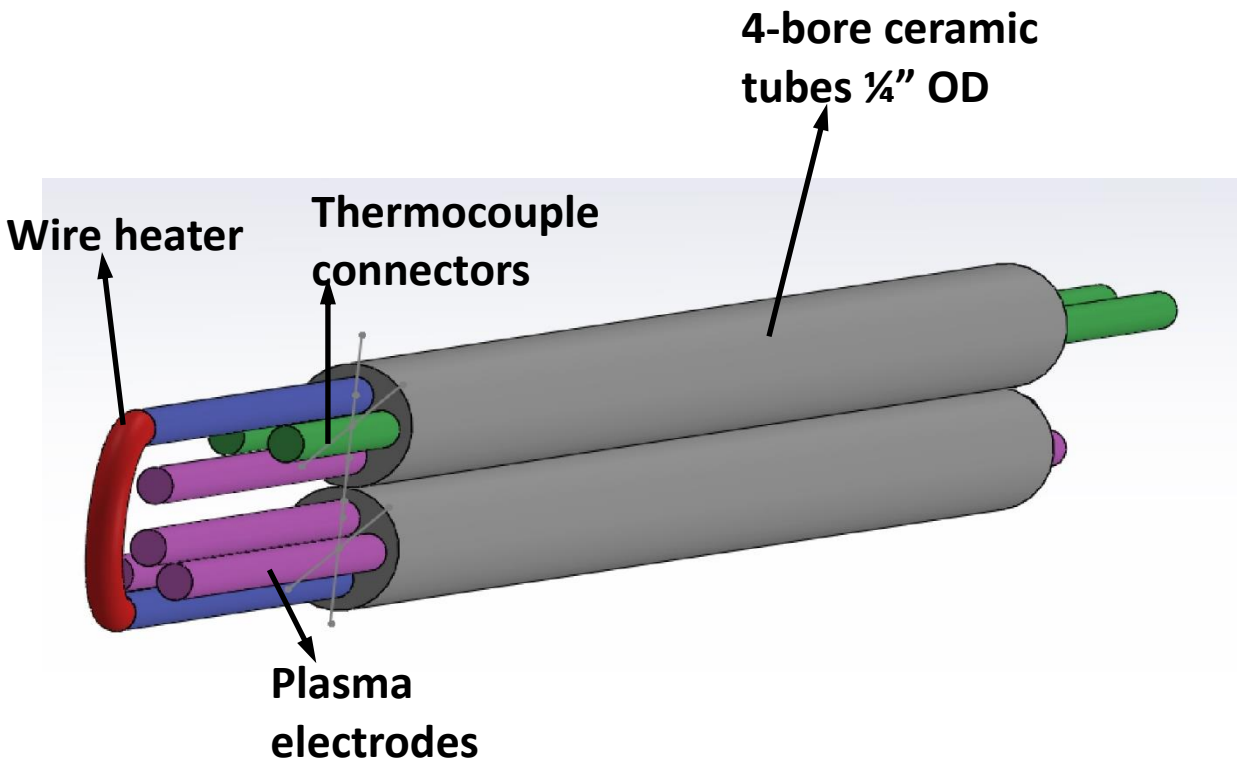

Figure 16: A drawing of the wire heater substrate assembly.

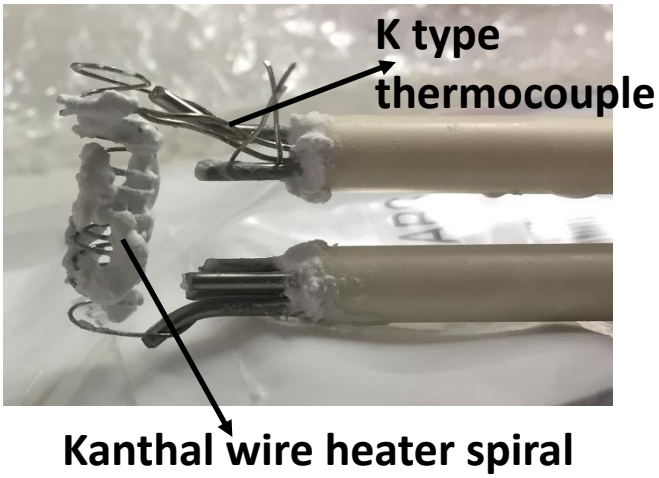

Figure 17: Picture showing the details of the spiral wire heater and attached thermocouple bead using electrically insulating ceramic adhesive.

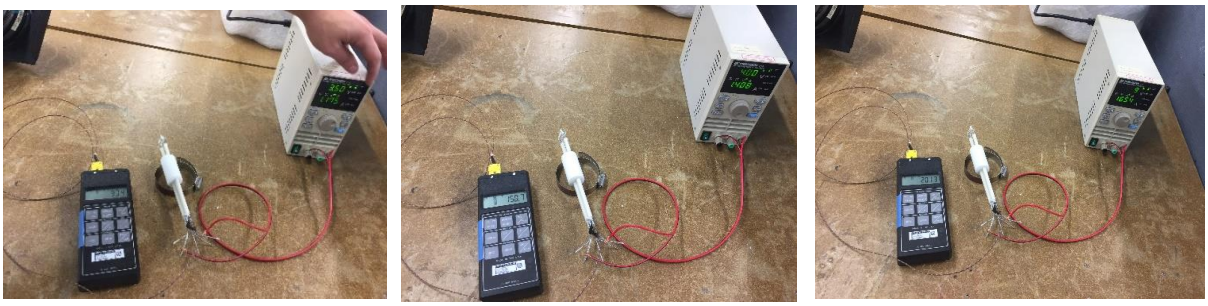

Figure 18: Testing of the wire heater and thermocouple using a DC power supply.

7. O atom concentration measurements by TALIF

Xe was used to calibrate the concentration of O atoms in the plasma. First, the TALIF signals from plasma was collected at various pressures and plasma powers. Then the plasma was turned off and the reactor was vacuumed. It was then filled with known concentrations of Xe. In our case we used 100 ppm Xe mixed with balance Ar as our calibration gas. Figure 12 shows an example Xe TALIF signal.

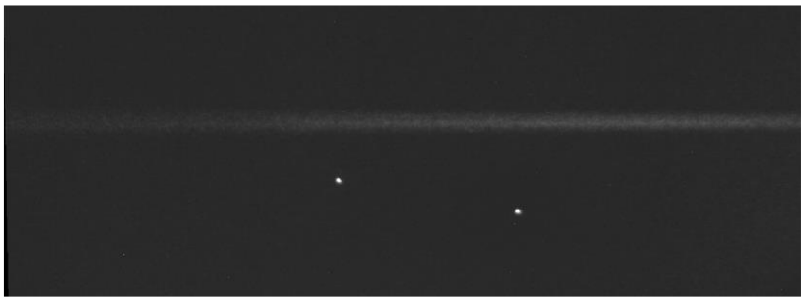

Figure 19: Xe atom TALIF signal`, 610 mTorr, partial pressure

Figure 21 shows the variation of the Xe TALIF signal with time. This was used to find the fluorescence lifetime of Xe.

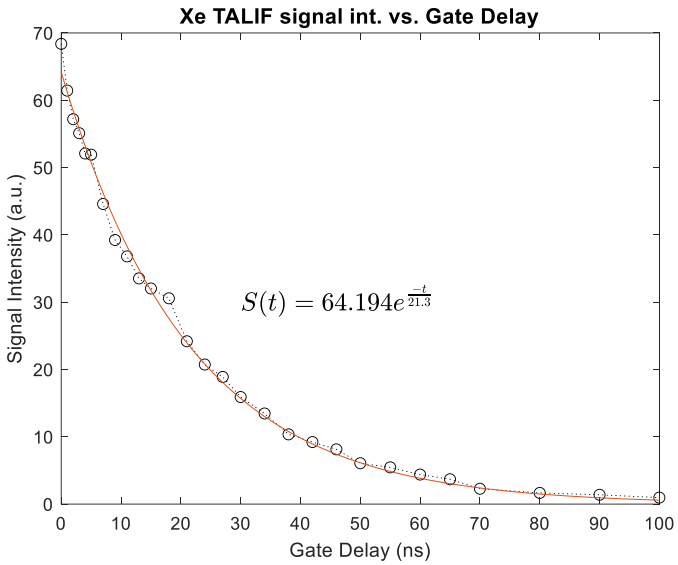

Figure 20: Variation of Xe TALIF signal with time, used to find the fluorescence lifetime.

The linearity region of Xe TALIF signal with square of the laser pulse energy was verified as shown in Figure 22. A laser pulse energy of 1-1.3 µJ/pulse was used in all our experiments to maintain signal linearity w.r.t atom or molecule concentrations being measured.

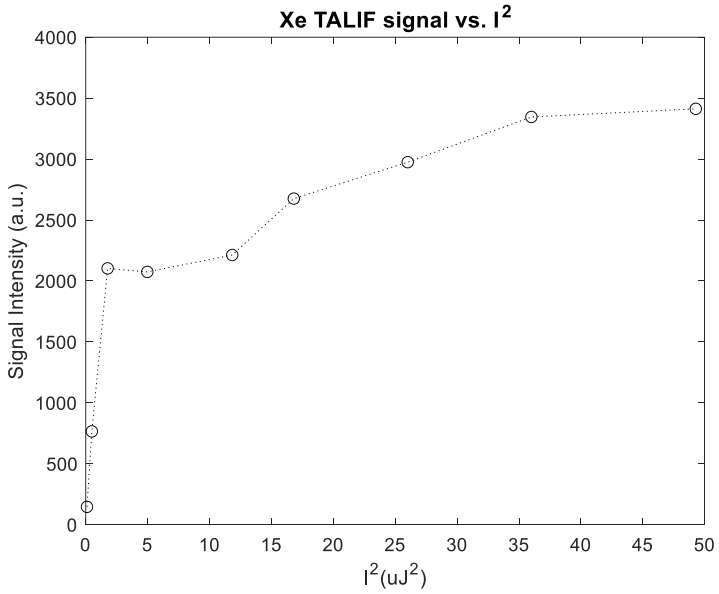

Figure 21: Variation of Xe TALIF vs. square of laser pulse energy, used to confirm linearity of TALIF signal.

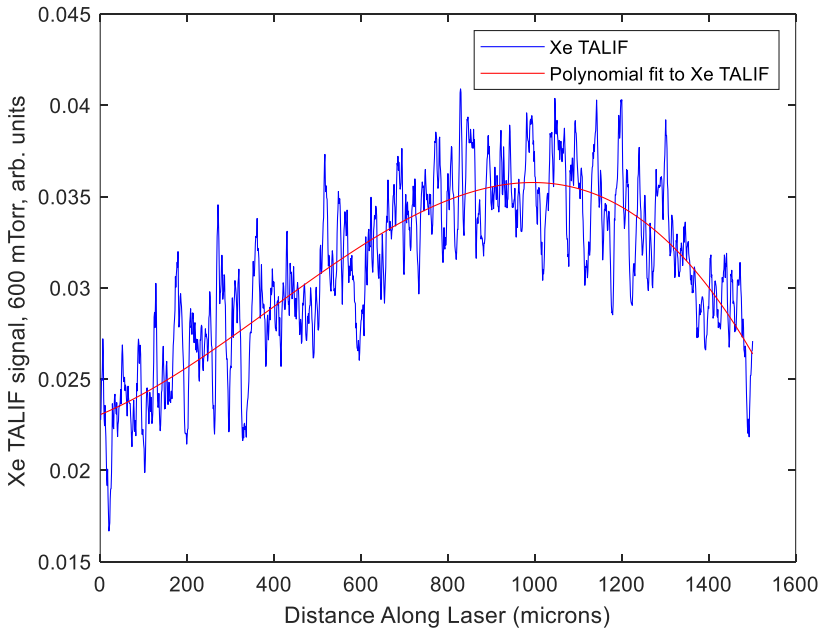

Figure 22: Measured Xe atom TALIF signal with distance. A smooth polynomial fit to the signal was used to calibrate the O atom density with spatial resolution.

Figure 13 (left) shows an example O atom TALIF signal. The ceramic substrate can be faintly seen in this picture to the right and vertical. Figure 13 (right) shows TALIF intensity averaged over the various rectangular pixels over the 2D TALIF signal collected as shown in Figure 13 (left) in red, green and blue.

From Figure 13 (right) it is found that the the TALIF signal intensity is linear w.r.t. square of laser pulse energy upt ~ 3 μJ/pulse (or 9 $(\mu J)^2$/pulse). In all our experiments, we used a pulse energy in the range 1-1.3 μJ/pulse to ensure linearity of signals w.r.t. atom/molecule concentrations.

Similarly, Figure 14 shows O atom TALIF signals at a higher pressure of 1040 mTorr and the linearity of signals was also verified as shown in Figure 15.

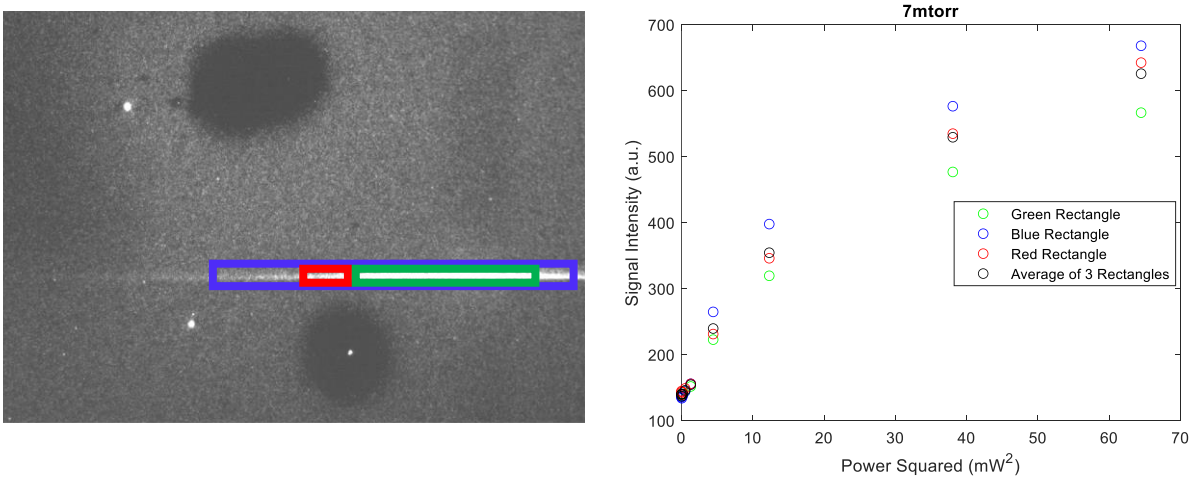

Figure 23: O TALIF signal 7 mTorr. 200x intensity, ceramic substrate.

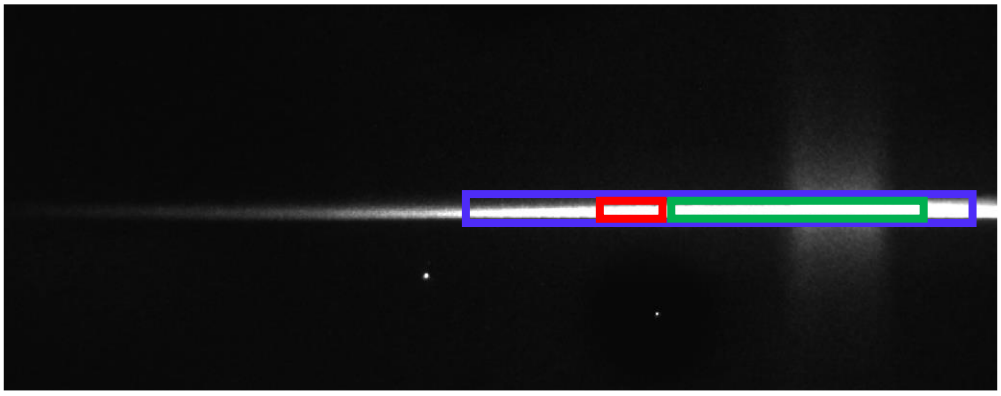

Figure 24: O TALIF signal 1050 mTorr. 20x intensity, ceramic substrate.

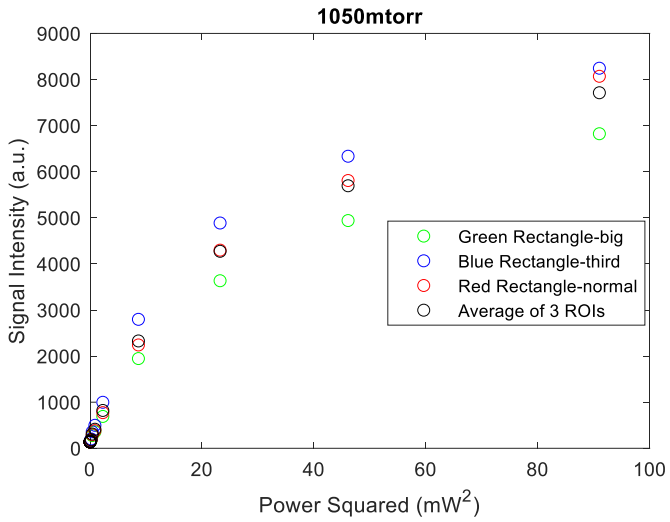

Figure 25: Variation of O atom TALIF signal vs square of laser pulse energy at 1050 mTorr, using different pixel regions of the LIF signal in Figure 14.

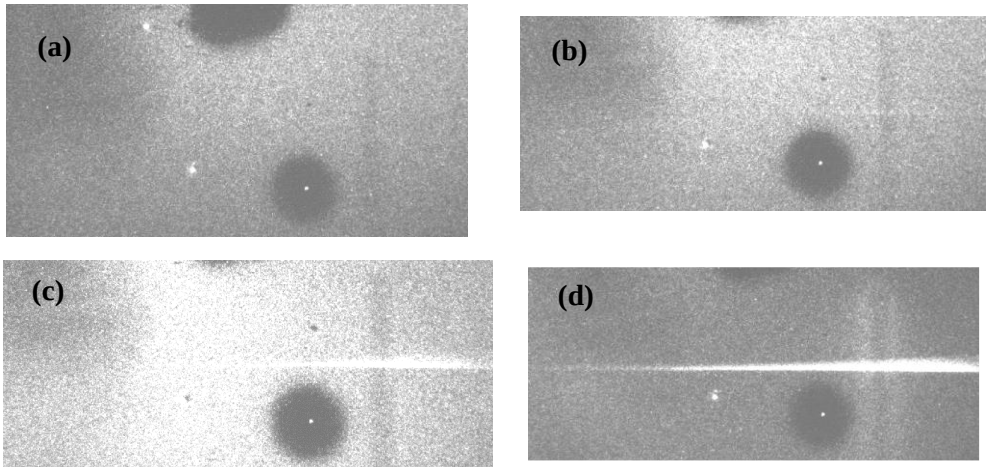

Figure 26: Variation (300x actual) of O atom TALIF signal in the ICCD images vs. pressure for 30 W plasma power (a) 4 mTorr; (b) 25 mTorr; (c) 104 mTorr; (d) 1048 mTorr.

Figure 16 shows the variation of O atom TALIF with pressure. The TALIF signals were found to increase with pressure as shown in Figure 23.

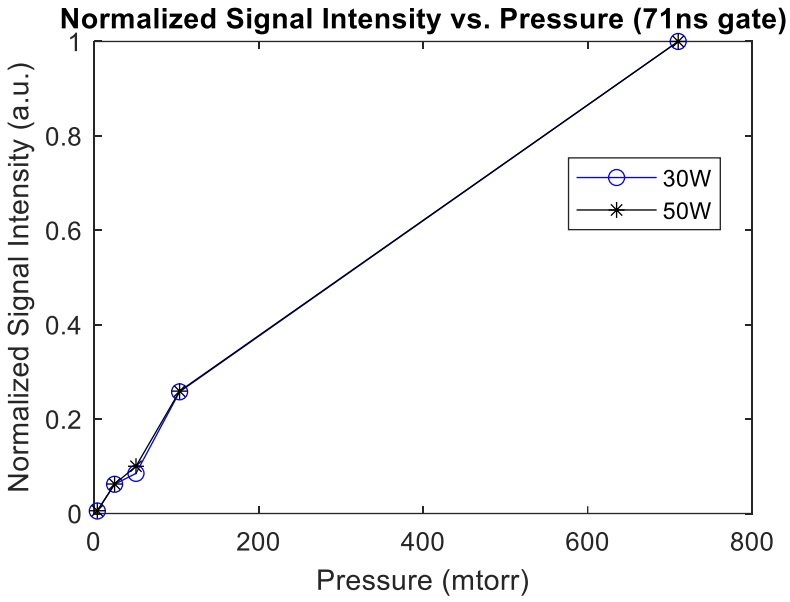

Figure 27: Variation of O atom TALIF vs. pressure for two different plasma powers.

Figures 24- 26 show the O atom concentration measurements over a metal substrate surface. Figures 27- 28 show the O atom concentration measurements over a ceramic substrate surface.

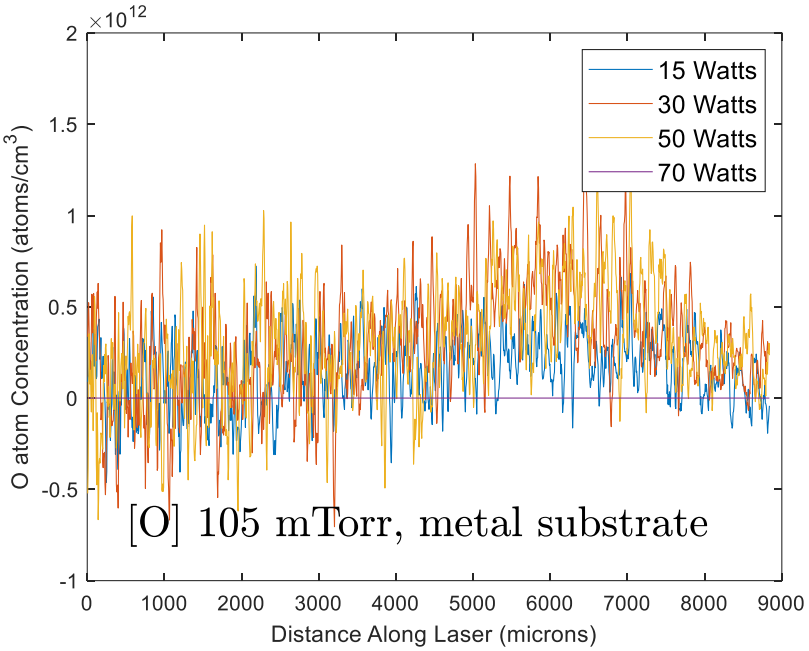

Figure 28: Measured O atom number density with distance.

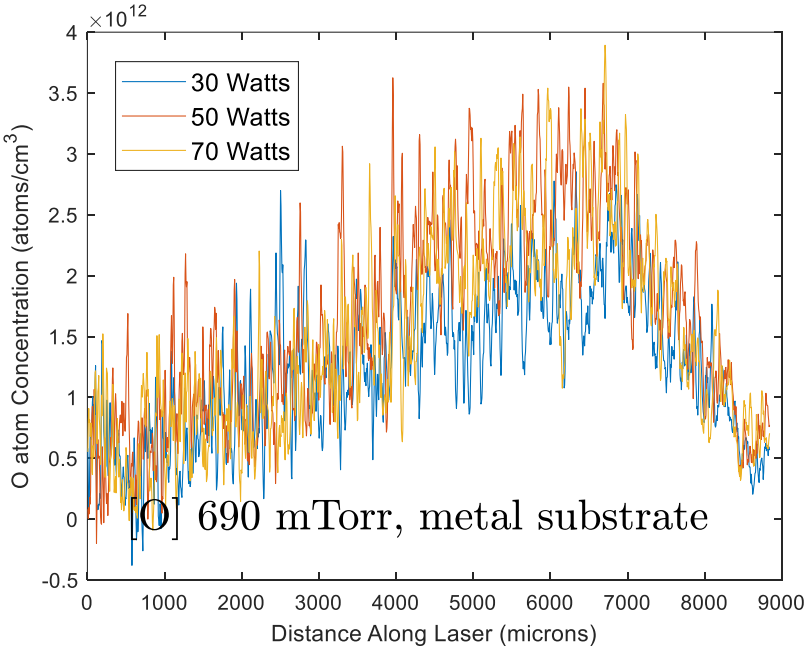

Figure 29: Measured O atom number density with distance.

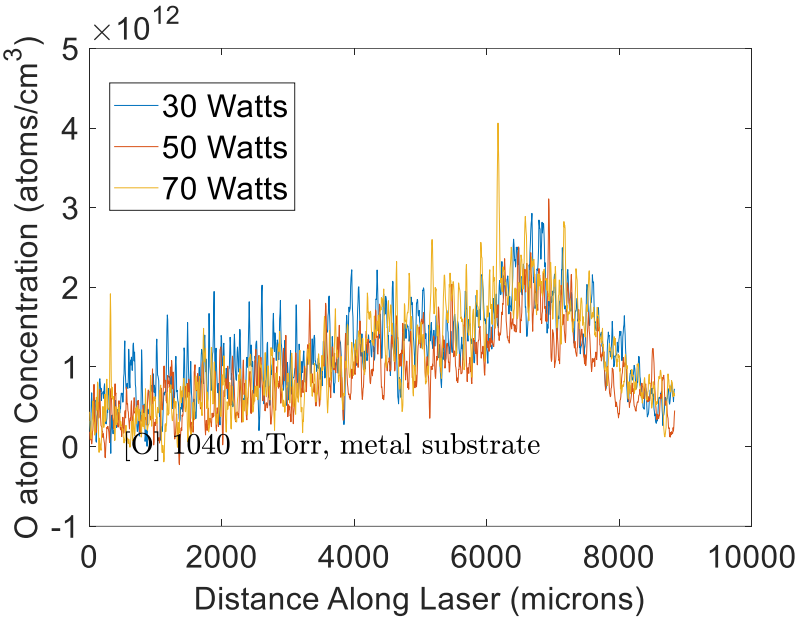

Figure 30: Measured O atom number density with distance.

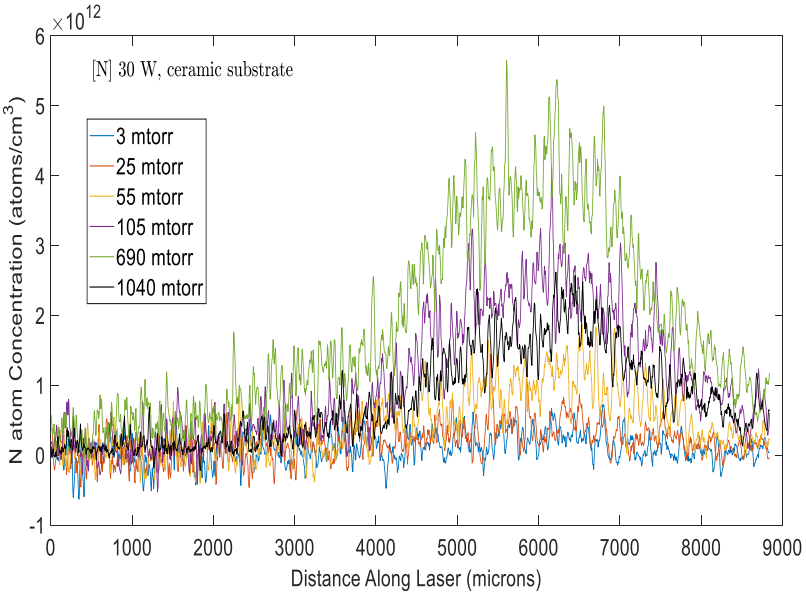

Figure 31: Measured O atom number density with distance.

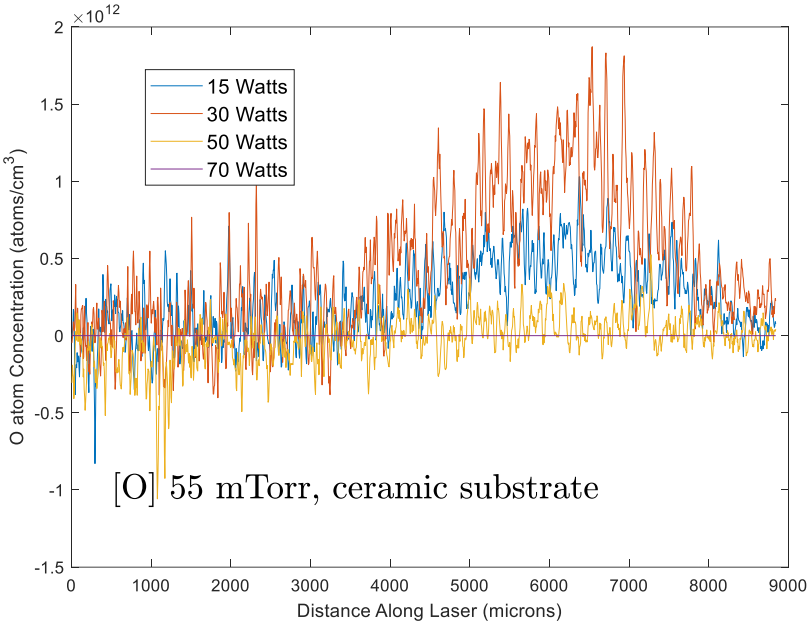

Figure 32: Measured O atom number density with distance.

8. N atom concentration measurements

Kr TALIF signal

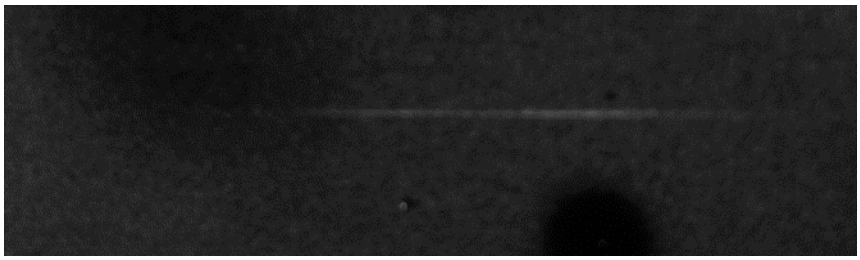

Figure 33: Kr TALIF signal along the laser line.

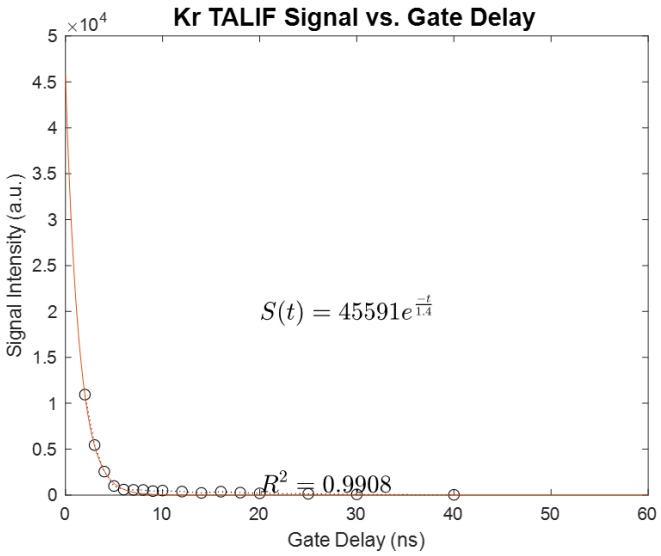

Figure 34: Kr TALIF signal variation vs. square of laser pulse energy, used to confirm linearity of signal.

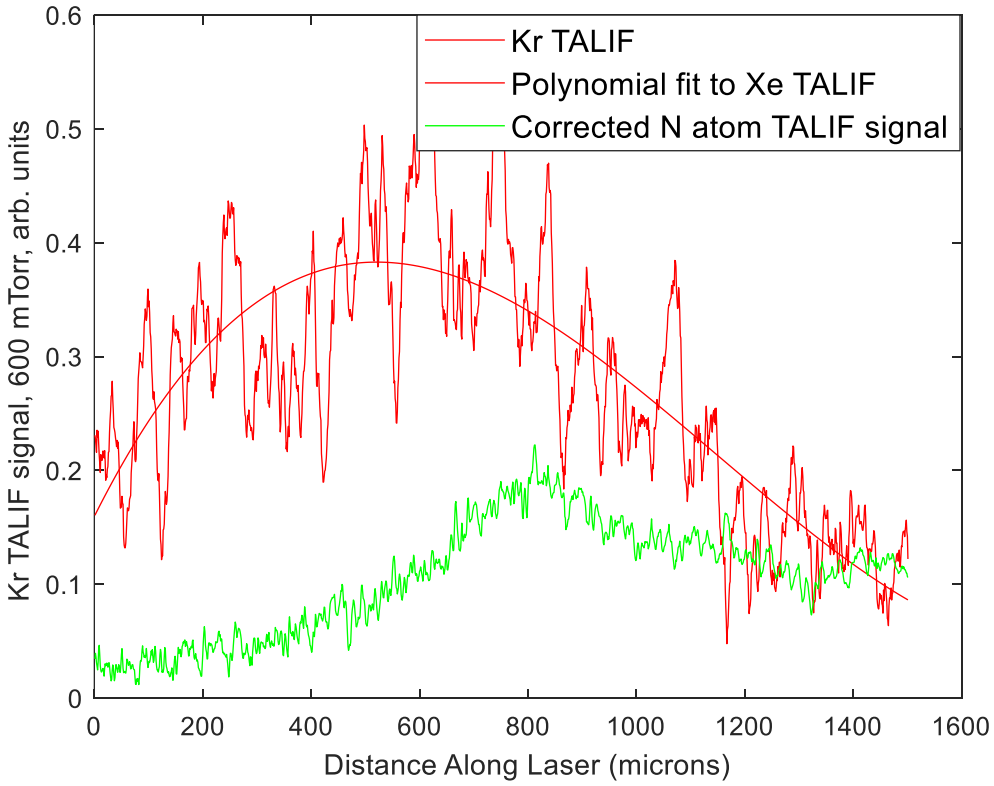

Figure 35: Measured Kr atom TALIF signal with distance. A smooth polynomial fit to the signal was used to calibrate the N atom density with spatial resolution.

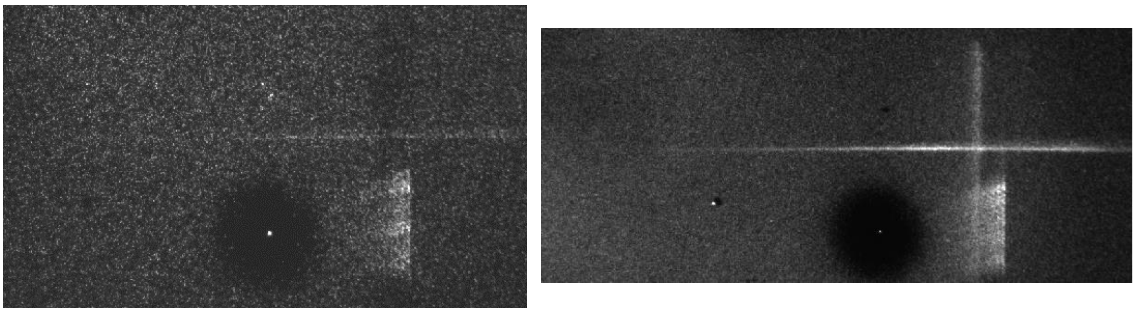

Figure 36: 50mtorr30W1ns
1055mtorr50W51ns

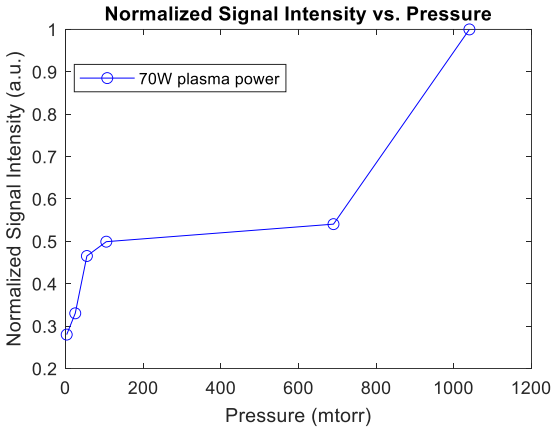

Figure 37: Variation of N atom TALIF signal with reactor pressure. Signal increased with pressure.

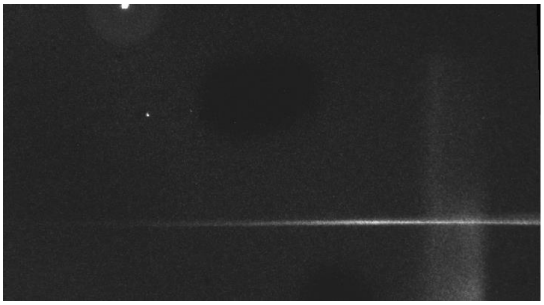

Figure 38: N atom TALIF signal over a ceramic substrate.

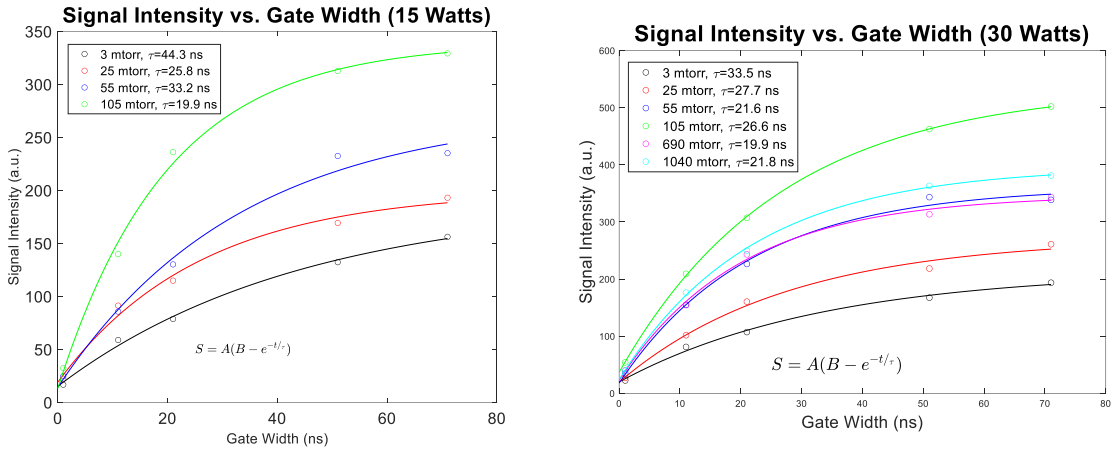

Figure 39: N atom TALIF signal vs time, used to find fluorescence lifetime. An averaged lifetime was used to estimate the N atom number densities.

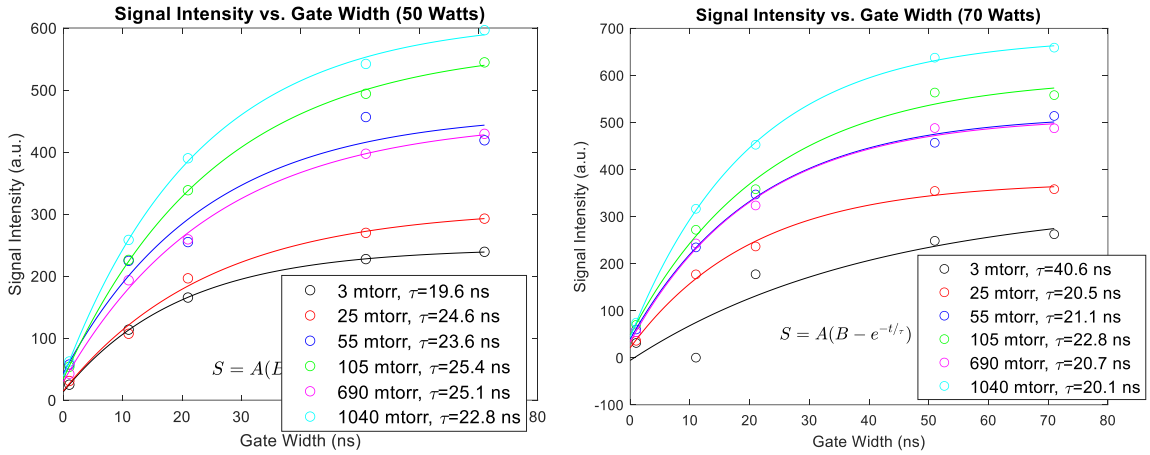

Figure 40: N atom TALIF signal vs time, used to find fluorescence lifetime. An averaged lifetime was used to estimate the N atom number densities.

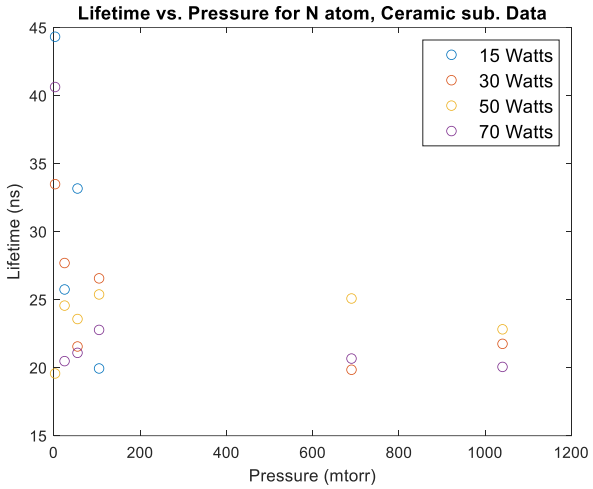

Figure 41: Variation of N atom TALIF signal lifetime

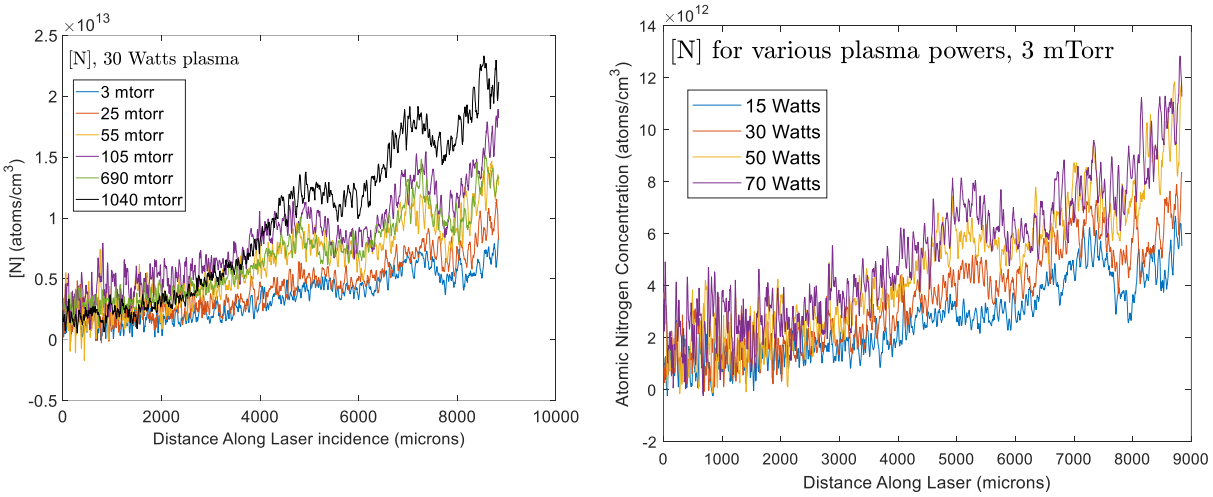

Figure 42: Measured N atom concentrations over a ceramic substrate

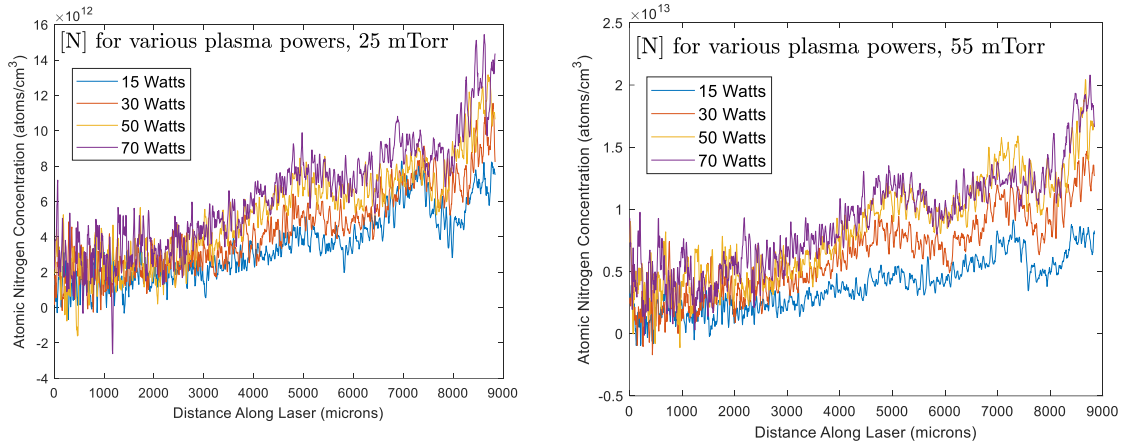

Figure 43: Measured N atom concentrations over a ceramic substrate

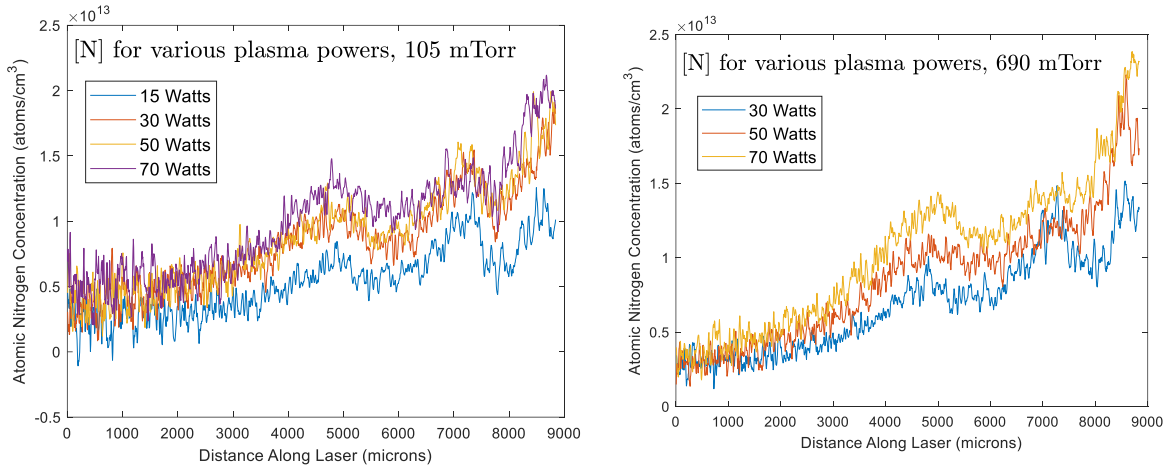

Figure 44: Measured N atom concentrations over a ceramic substrate

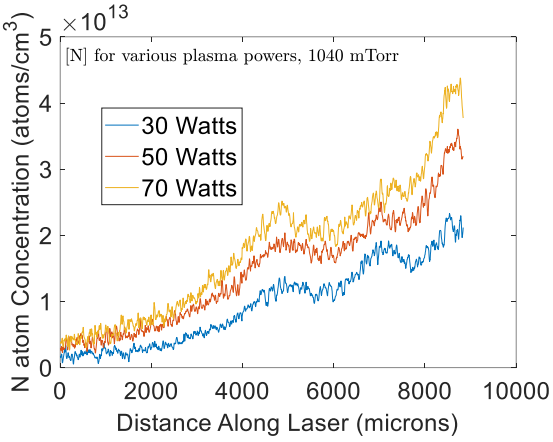

Figure 45: Measured N atom concentrations over a ceramic substrate

Measurements over metal substrate

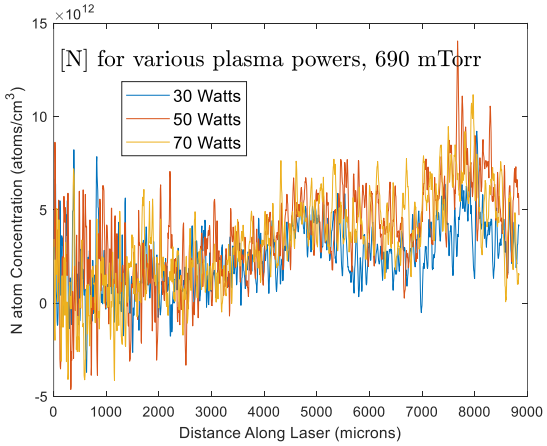

Figure 46: Measured N atom concentrations over a metal substrate

9. NO concentration measurements by LIF

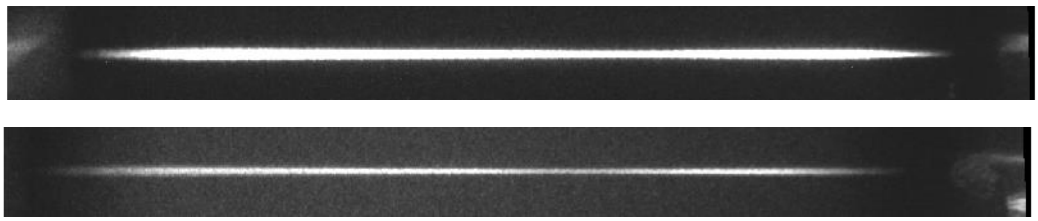

Figure 47: NO LIF signal variation with laser pulse energy. The LIF signal is found to be mostly linear w.r.t laser energy below ~ 4 µJ/pulse.

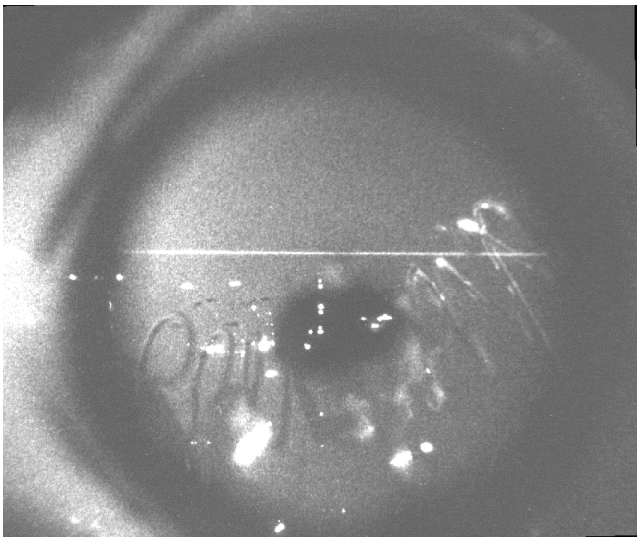

Figure 48: NO LIF signal along the laser path. Laser passed with grazing incidence over the wire heater to the right.

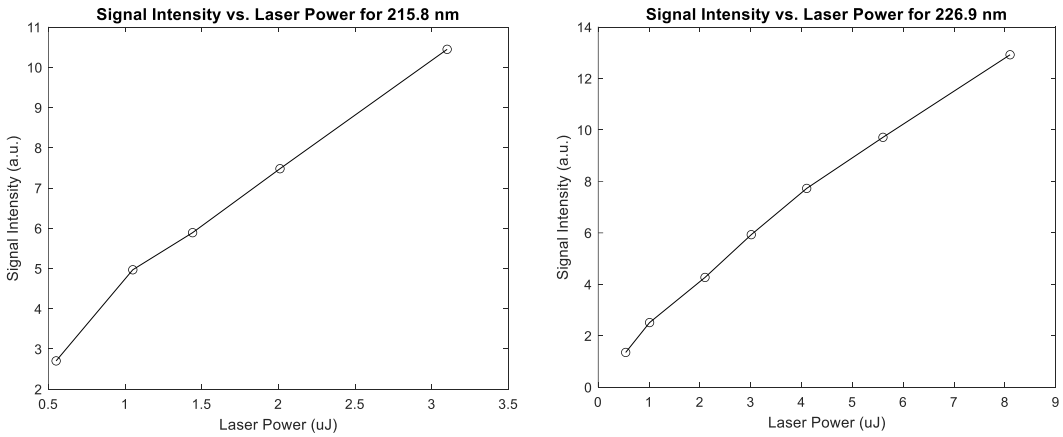

Figure 49: NO LIF signal variation with laser pulse energy. The LIF signal is found to be mostly linear w.r.t laser energy below ~ 4 µJ/pulse.

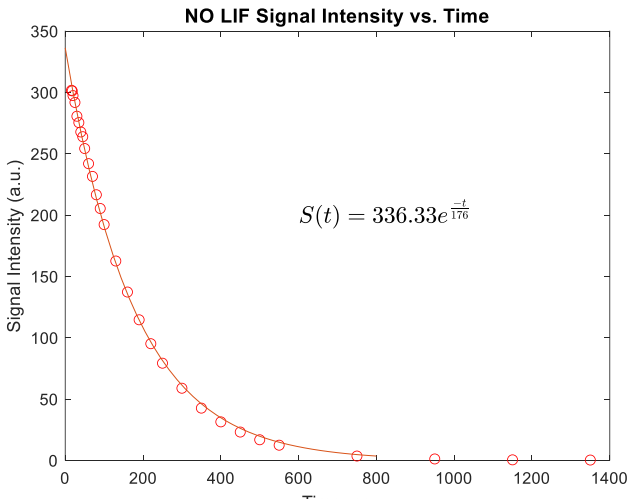

Figure 50: NO LIF signal variation with time, used to find the fluorescence lifetime.

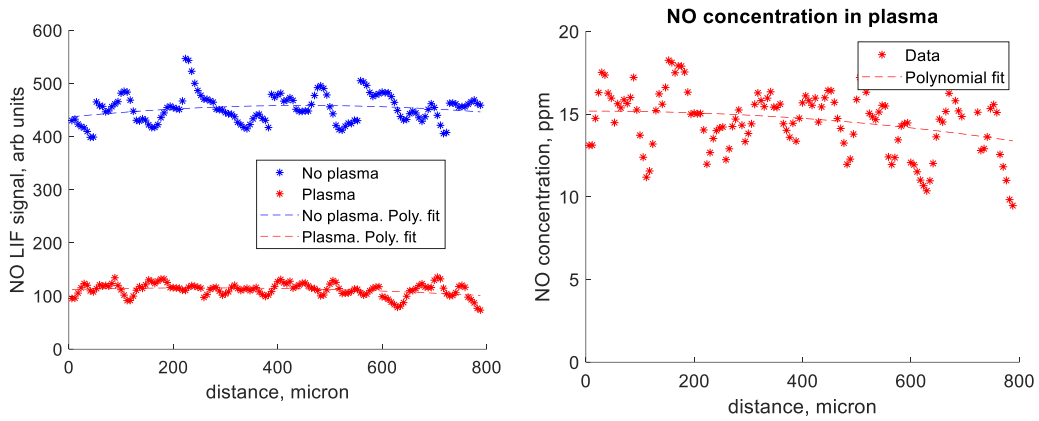

Figure 51: (a) NO LIF signal at 226 nm from calibration NO gas (2% NO + N2 balance) vs distance, total pressure 125 mTorr, room temperature of 298 K; (b) measured NO concentration in plasma vs distance in 16 W plasma, 109 mTorr total pressure air flow, at 226 nm.

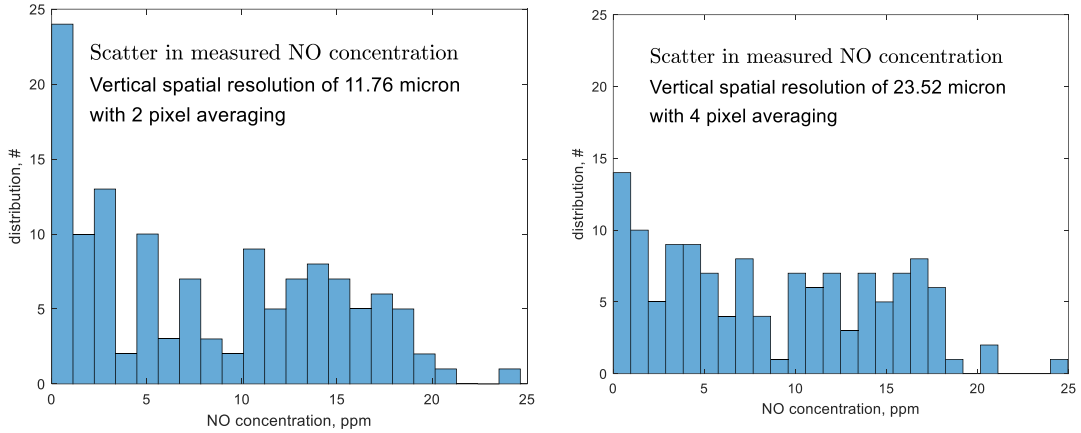

Figure 52: Scatter in measured NO concentrations vs. spatial resolution achieved

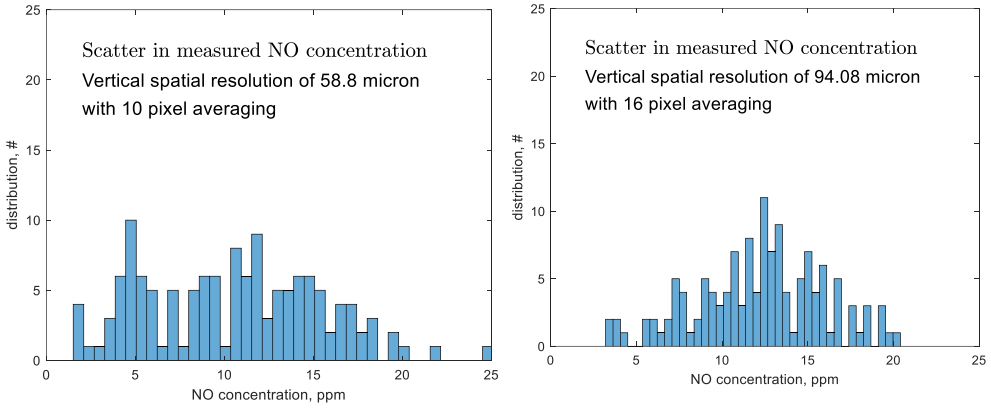

Figure 53: Scatter in measured NO concentrations vs. spatial resolution achieved

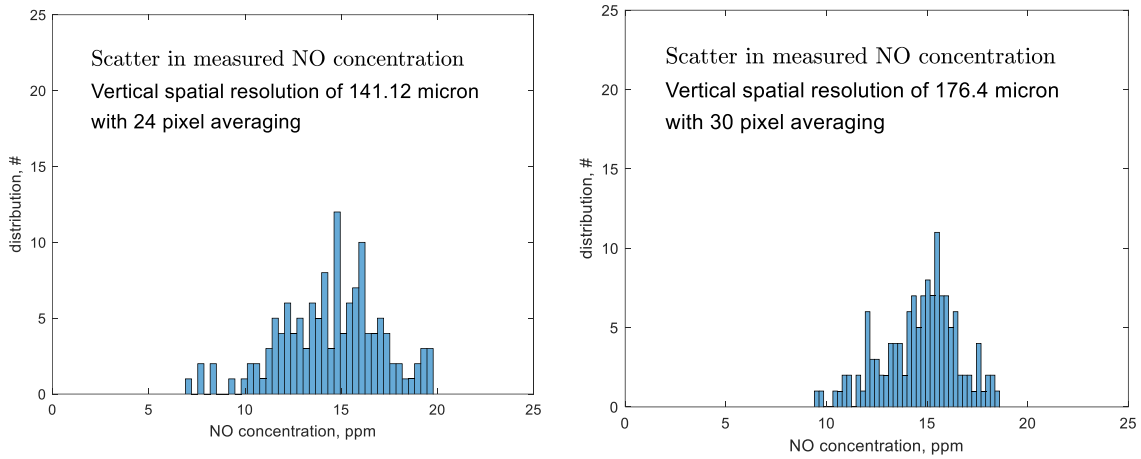

Figure 54: Scatter in measured NO concentrations vs. spatial resolution achieved

10. Temperature measurements using NO PLIF imaging

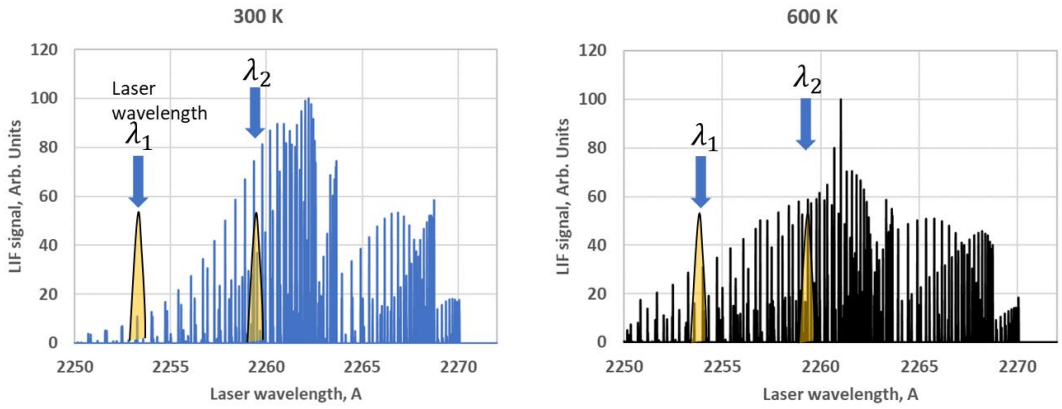

Figure 55: NO LIF excitation spectrum for two different temperatures, 300 K and 600 K. The ratio of fluorescence at two wavelengths changes with temperature and is independent of NO concentration, provided the LIF signal is not saturated with high laser energy or high NO concentrations. LIFBASE was used to simulate the spectrum.

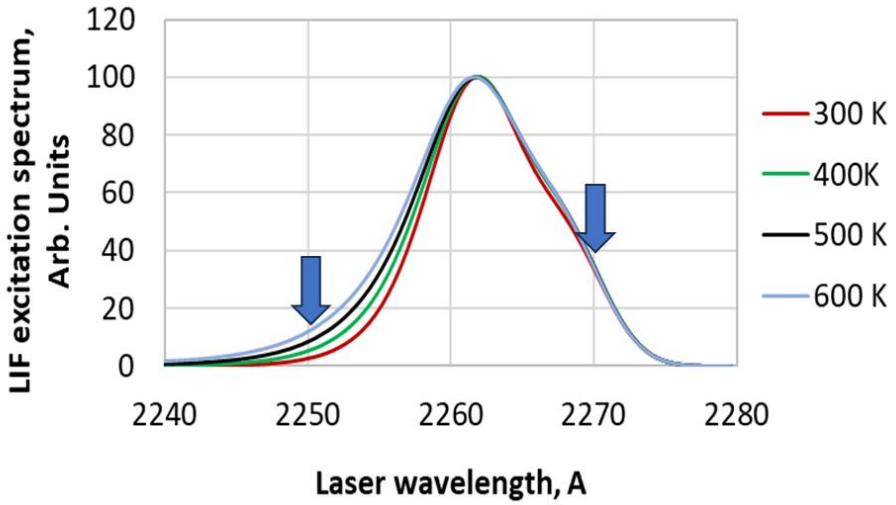

Figure 56: For a wider laser linewidth such as for femtosecond laser, the finer features in the NO LIF excitation spectrum is lost. However, the fluorescence ratio sensitivity to temperature at the two wavelengths 225 nm and 227 nm is still observed. This variation was used to measure temperature over a surface using NO PLIF imaging.

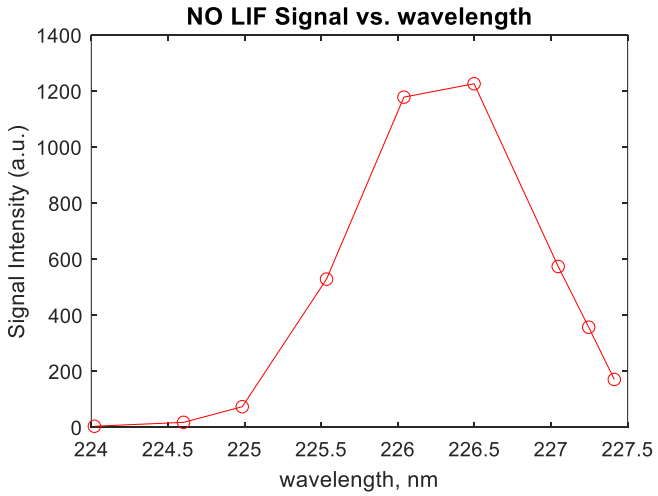

Figure 57: Measured NO LIF signal variation with wavelength using the wider linewidth ~ 1 nm femtosecond laser at TAMU.

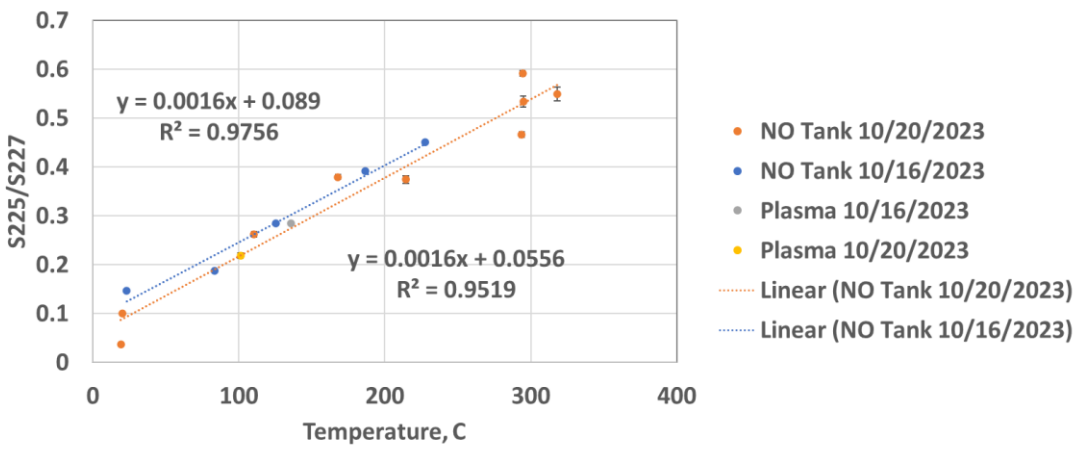

Figure 58: Measured temperatures using NO PLIF imaging, first with reactor filled with NO and then with air plasma generated NO.

11. Summary

The proposed measurements of concentrations of O atoms and temperatures using NO PLIF imaging over metal and ceramic substrates have been completed. Additionally, N atom and NO molecule concentrations were also measured in the plasma over the solid substrate surfaces.

To our knowledge we measured temperatures using NO PLIF imaging using femtosecond laser for the first time. The uncertainty in temperature is found to be ~ ± 15 K.

The concentrations of N and O atoms were found to be in the range of 10^{12} – 10^{13} atoms/cc, which was in reasonable agreement with literature.

The measured NO concentrations were in the range of 10-20 ppm in plasma.

The TALIF and LIF signals increased with pressure, which is reasonable, because of increased density of gas.

There is a trade-off between desired spatial resolution and the signal to noise ratio in the measurements. However, more analysis and algorithms to average the pixel intensities to achieve a good trade-off between spatial resolution and scatter in measured concentrations is required.

The spatial resolution in our imaging can be further improved by including a > 10 x microscope in our imaging. A spatial resolution of better than 10 µm along with better S/N ratio is possible with this approach, which can be developed in Phase II.

In the absence of NO, temperature measurements can be done using other molecules present in the plasma, which will be the focus of study in Phase II.

12. Dissemination of results to communities of interest

1. Submitted abstract for poster session and oral presentations to 3 conferences:

   https://ald2023.avs.org/
   Title: Laser diagnostics of plasma surface interactions
   Conference dates: Sunday, July 23-Wednesday, July 26, 2023
   Location: Bellevue (near Seattle), Washington, USA

   https://avs69.avs.org/abstract-submission/
   Title: In-situ laser diagnostics of plasma surface interactions by fs-TALIF
   Conference dates: 5-10 November, 2023
   Location: Portland, OR

   AIAA SciTech 2024
   https://www.aiaa.org/scitech
   Title: Fs-TALIF for Low Pressure Interfacial Plasmas
   Conference dates: 8-12 January, 2024
   Location: Orlando, FL

13. Future Work

- Complete analysis of the data
- Prepare manuscript for article publication.
- Apply for Phase II
- Explore commercialization and development of new methods of plasma processing.

14. Impacts

The research provided opportunities to train new hire technicians, graduate students (Mr. Gerardo Urdaneto), summer undergraduate intern (Mr. James Montoya), undergraduate students and other engineers at ACT and TAMU.

15. Changes

"Nothing to Report."

16. References

1. Boris, D. R. *et al. J. Vac. Sci. Technol. A* 38, 040801 (2020).
2. Faraz et al., Energetic ions during plasma-enhanced atomic layer deposition and their role in tailoring material properties, Plasma Sources Sci. Technol. 28 (2019) 024002 (19pp).
3. *Plasma Science for Microelectronics Nanofabrication*, DOE Fusion Energy Sciences (FES) Workshop on Plasma Science for Microelectronics Nanofabrication, August 8-9, 2022, Gaithersburg, MD.